AIP | Applied Physics Letters

Direct measurement of neutral gas heating in a radio-frequency electrothermal plasma micro-thruster

A. Greig, C. Charles, R. Hawkins, and R. Boswell

Citation: Appl. Phys. Lett. **103**, 074101 (2013); doi: 10.1063/1.4818657
View online: http://dx.doi.org/10.1063/1.4818657
View Table of Contents: http://apl.aip.org/resource/1/APPLAB/v103/i7
Published by the AIP Publishing LLC.

Direct measurement of neutral gas heating in a radio-frequency electrothermal plasma micro-thruster

A. Greig,[1,a)] C. Charles,[1] R. Hawkins,[1,2] and R. Boswell[1]
[1]*Space Plasma, Power and Propulsion Laboratory, Research School of Physics and Engineering, The Australian National University, Canberra ACT 0200, Australia*
[2]*Supercomputer Facility, The Australian National University, Canberra ACT 0200, Australia*

(Received 17 April 2013; accepted 1 August 2013; published online 13 August 2013)

Direct measurements and modelling of neutral gas heating in a radio-frequency (13.56 MHz) electrothermal collisional plasma micro-thruster have been performed using rovibrational band matching of the second positive system of molecular nitrogen (N_2) for operating pressures of 4.5 Torr down to 0.5 Torr. The temperature measured with decreasing pressure for 10 W power input ranged from 395 K to 530 K in pure N_2 and from 834 K to 1090 K in argon with 1% N_2. A simple analytical model was developed which describes the difference in temperatures between the argon and nitrogen discharges. © *2013 AIP Publishing LLC*. [http://dx.doi.org/10.1063/1.4818657]

Although mono- or bi-propellant chemical thrusters are the basis of space propulsion, electric thrusters have become more prevalent over recent years with several hundred now in operation on commercial satellites.[1–3] Micro-satellites, generally with a total weight less than 120 kg, require low power, small, lightweight micro-thrusters. Presently, the majority of micro-thrusters in use are cold gas thrusters or resistojets. Cold gas thrusters, while not technically an electric thruster, are the simplest form of propulsion where an inert gas is expelled through a nozzle. However, as there is no combustion or heating of the gas, thrust produced per kilogram of propellant is low. Resistojets heat propellant through contact with heated walls or a coil[1,4] but this leads to shortened lifetimes due to thermal fatigue and requires power on the order of 10^2 W.

Recently a low power radiofrequency (rf) capacitively coupled plasma (CCP) micro-thruster, known as "Pocket Rocket" has been discussed.[5–7] The 20 mm long, 4.2 mm-diam discharge operates at pressures around a few Torr and is weakly ionized (less that 1%).[6] Typical plasma densities[6] for a 1.5 Torr argon plasma have been estimated at 2×10^{12} cm^{-3}. However, ions in the discharge would typically reach a Bohm velocity on the order of a few thousand ms^{-1}, an order of magnitude greater than a typical thermal gas velocity of a few hundred ms^{-1}, and ion-neutral charge exchange collisions would yield neutral gas heating within the discharge, hence thrust. It is expected the majority of ion-neutral charge exchange collisions are occurring within the main plasma bulk inside the discharge tube, with collisions continuing into the expansion plume region downstream of the thruster, with decreasing frequency as distance from the tube increases.[8]

Thrust from collisional plasmas has been analytically discussed by Fruchtman[9] and referred to as "neutral pumping" which is effectively neutral gas heating. The qualitative results are in agreement with the development of "Pocket Rocket" as a potential rf electrothermal collisional plasma micro-thruster. Power balance calculations relating the input power to discharge velocity (assuming 100% efficiency) reported an estimated neutral gas temperature of 1430 K for a 10 W, 1.5 Torr argon plasma.[6] Here direct measurements of neutral gas heating are carried out using optical emission spectroscopy (OES) and a basic model of gas heating is derived for atomic and molecular gases.

The Pocket Rocket device, previously described in depth,[6] is shown in its present form in Figure 1, consisting of a 4.2 mm inside diameter, 1 mm thick, 20 mm long alumina sleeve connecting an upstream plenum cavity and downstream expansion tube. Constant rf power of 10 W at 13.56 MHz is capacitively coupled into the plasma through a copper rf electrode surrounding the sleeve at the midpoint, with two grounded aluminium electrodes placed at either end of the tube. The discharge gas, pure nitrogen (N_2) or argon with 1% N_2, is injected through the plenum chamber with operating plenum pressures ranging from 0.5 Torr to 4.5 Torr.

The plenum cavity has a rear view port to allow optical diagnostics of the discharge. Digital images, captured using a digital camera in conjunction with a bandpass filter looking through the view port, give radial intensity profiles of visible emission lines across the discharge diameter. Depending on the ionization model for the emission line imaged, the radial distribution of electrons can be determined. The OES system consists of a SPEX 500 M monochromator with 50 μm slit width and 1200 groove/mm grating used in conjunction with a 4 mm diameter fused silica fiber-optic cable to direct light from the discharge onto an Ames Photonics Garry 3000 S charged couple device (CCD) array. The CCD array captures a 34 nm wavelength range spectra with 0.02 nm resolution. The optical fiber was positioned looking though the plenum view port directly down the alumina sleeve. As the optical fiber diameter is approximately the same as the discharge diameter, the resulting spectra are spatially averaged over the discharge volume.

The non-invasive OES method used to determine the neutral gas temperature of the discharge involves fitting computer generated spectra to experimentally determined rovibrational band spectra, produced by electronic transitions from upper states (denoted by $'$) to lower states (denoted by $''$) of diatomic molecules. The fitting estimates the rotational temperature of the discharge gas, which is

a)Electronic Mail: amelia.greig@anu.edu.au

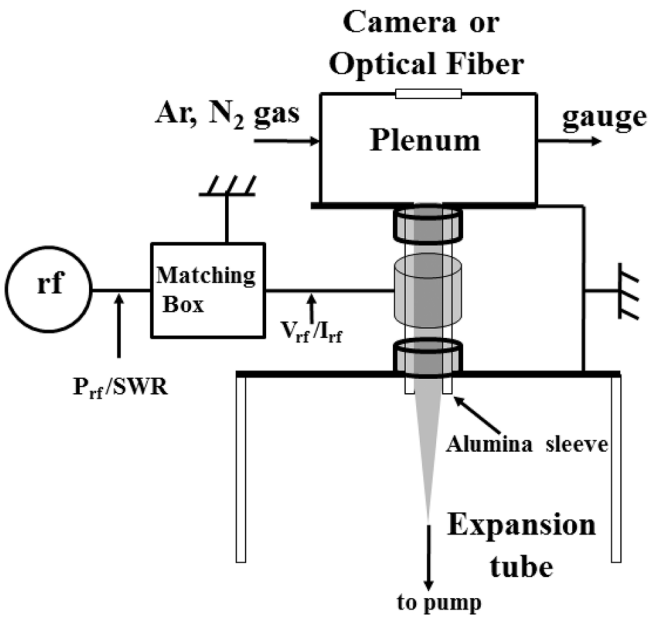

FIG. 1. Experimental setup of the Pocket Rocket plasma system.

approximately equal to the neutral gas temperature for the conditions tested.[10] This technique has been previously used to determine the temperature of discharges ranging from atmospheric pressure[11] to around a Torr.[12,13] Atomic species do not produce rovibrational bands as no rotational and vibrational modes exist. An alternate spectroscopic method for determining gas temperature, including directly from atomic species, is Doppler broadening where the change in width of a spectral line is measured to infer temperature.[14] However, for this discharge, an estimated temperature increase of 1000 K results in an increase in line width of the order of 1 pm, below the equipment resolution of 20 pm, hence this method cannot be used. Therefore, to use the rovibrational OES technique for an argon plasma, trace amounts of N_2 (~1%) were added to the discharge instead.

The second positive system of N_2 ($C^3\Pi_u \rightarrow B^3\Pi_g$) in the wavelength region 372–381 nm to include the (0,2) and (1,3) vibrational transitions was chosen for this work as this region presents minimal interference from strong argon lines and the required constants are readily available. The (2,4) and (3,5) vibrational transition intensities were too low for some pressures tested to allow a fitting, so for consistency these transitions were omitted. Generation of the simulated spectra is achieved by calculating the wavelengths of the required transition lines and the related intensities, then broadening the lines to match the experimentally determined spectra.[10] The wavelength (λ) of an electronic transition from the $Cv'J'$ to $Bv''J''$ state is

$$\lambda^{Cv'J'}_{Bv''J''} = \left[n_a \sum_{pq} Y^C_{pq} \left(v' + \frac{1}{2} \right)^p [J'(J'+1)]^q - Y^B_{pq} \left(v'' + \frac{1}{2} \right)^p [J''(J''+1)]^q \right]^{-1}, \quad (1)$$

where J represents the rotational state, v represents the vibrational state and n_a is the refractive index of air. The constants Y_{pq} are Dunham coefficients[15] taken from Bai *et al.*[12] For each wavelength calculated, the intensity of the spectrum is determined using

$$I^{Cv'J'}_{Bv''J''} = \frac{D}{\lambda^4} q_{v',v''} e^{\frac{-E_{v'}}{kT_v}} S_{J',J''} e^{\frac{-E_{J'}}{kT_r}}, \quad (2)$$

where D is an arbitrary scaling constant, k is Boltzmann's constant, $q_{v',v''}$ are Franck-Condon factors (taken from Zare *et al.*)[16] and $S_{J',J''}$ are Holn-London factors calculated from Herzberg[17] (p. 208). The rotational energy ($E_{J'}$) and vibrational energy ($E_{v'}$) are also calculated from Herzberg[17] (pp. 106–107, 552).

A Gaussian convolution kernel was used to broaden the simulated spectral lines to match the equipment based line broadening of the experimental spectra. An example fit between experimental data and simulated spectrum is shown in Figure 2 for a 10 W argon plasma with 1% N_2 addition at 1.5 Torr. Monte Carlo Markov chains were used for fitting the experimental and simulated data resulting in a range of credible values for T_r. For this example fit, the estimated temperature was 1090 ± 35 K. Weak argon lines produced minor interference at 373.8 nm, 376.5 nm, and 378.1 nm and slightly enhanced rotational tail structures at lower wavelengths were caused by excess kinetic energy from Ar-N_2 collisions being transferred into higher rotational states for both vibrational bands.[18] The estimated experimental error is ± 50 K based on repeatability of results giving a neutral gas temperature estimate of 1090 ± 85 K for a 10 W, 1.5 Torr argon discharge, which is lower than, but of the order of, the gas temperature estimated through power balance calculations discussed previously[6] (~1430 K). The power balance calculations assumed 100% efficiency, whereas the experimental power transfer efficiency would be considerably lower, explaining the difference between the two temperature values.

Applying this method to pure N_2 and argon (with 1% N_2) discharges at 10 W for pressures ranging from 0.5 Torr to 4.5 Torr gave estimated neutral gas temperatures as shown in Figure 3. The temperature of the N_2 plasma decreased from 430 K to 360 K as pressure increased from 0.5 to 4.5 Torr. The temperature of the argon plasma is consistently 600–700 K (or about 2.2–2.5 times) higher than the N_2 plasma for all pressures tested with temperatures ranging from 780 K to 1120 K. Comparing these results to other works, Huang *et al.*[13] found gas temperatures between 350 K and 600 K for a 5 to 200 W mTorr dual frequency N_2 CCP discharge and Bai, Swann, and Cruden[12] found gas temperatures around 1860 K for a transformer coupled argon discharge between 0.5 and 1 Torr at 1.6 kW. Interestingly, comparison of the results to atmospheric pressure plasma jet (APPJ) works with similar geometries to the Pocket Rocket

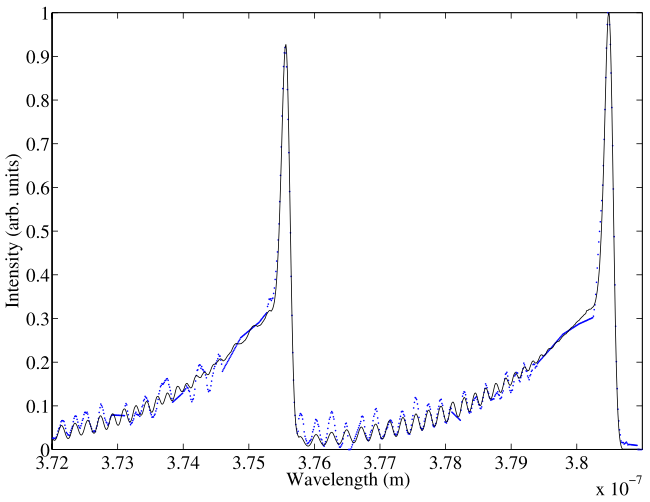

FIG. 2. Example of experimental and simulated spectra fit for a 10 W, 1.5 Torr Ar plasma with 1% N_2 addition. The experimental data points are shown as closed blue circles, the simulated spectrum overlayered as a solid black line.

device but with smaller discharge diameters and different discharge gases gave very different results, with air mixtures usually reaching higher temperatures than noble gas discharges of Helium and Neon,[19,20] suggesting gas mixture, pressure, discharge cavity dimensions, and power density play a large role in the gas temperatures achieved.

To understand the difference in temperatures between the N_2 and argon discharges, a simplistic model of the neutral gas heating mechanism was developed. The ionization energies of argon (Ar) and N_2 are 15.76 eV and 15.58 eV, respectively, giving 0.18 eV of excess energy during an Ar-N_2 ion-neutral charge exchange collision, three orders of magnitude lower than the translational kinetic energy of the ion. As the N_2 trace comprises only 1% of the total discharge gas the resulting effects are expected to be negligible and the argon with 1% N_2 discharge model was based on pure argon.

During an ion-neutral charge exchange collision with a low energy ion, it is assumed that half the kinetic energy (KE) is transferred from the hot ion to the cold molecule,[21]

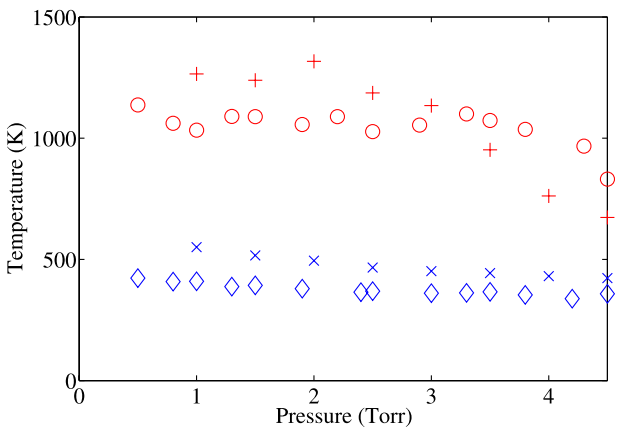

FIG. 3. Experimental neutral gas temperatures for Ar with 1% N_2 trace added (open red circles) and N_2 (open blue diamonds) discharges for pressures ranging from 0.5 Torr to 4.5 Torr with 10 W power input. Estimated neutral gas temperatures for Ar (red plus symbols) and N_2 (blue crosses) discharges for pressures ranging from 1 Torr to 4.5 Torr using a simplistic model based on collisional and kinetic effects.

with $KE = \frac{1}{2}mv^2$ where m and v are the molecules mass and velocity, respectively. The initial KE of the ions is based on the Bohm velocity (v_B), calculated using $v_B = \sqrt{\frac{eT_e}{m}}$, where e is the electron charge, T_e is the electron temperature, and m is the ion mass. The electron temperature was taken as 2.5 eV for both Ar and N_2, based on previous reports,[6] giving $v_{B_{Ar}} = 2450\,\mathrm{ms}^{-1}$ and $v_{B_{N_2}} = 2930\,\mathrm{ms}^{-1}$. The KE for an n-degree of freedom molecule is $\frac{n}{2}kT$, where T is the temperature of the molecule. Argon gas contains atomic molecules with three translational degrees of freedom to store energy ($n_{Ar} = 3$), while nitrogen gas contains diatomic molecules with three translational, two rotational, and one vibrational degrees of freedom ($n_{N_2} = 6$), resulting in overall lower temperatures for N_2 when compared with Ar for the same collisional KE transfer. This gives estimates of 4980 K and 2640 K for the temperature of the hot neutrals after the ion-neutral charge exchange collision for Ar and N_2, respectively. However, as the discharge is weakly ionized not all cold neutrals undergo a charge exchange collision with a hot ion. Ionization fractions ($\frac{n_i}{n_g}$) were calculated from ion saturation currents (I_{sat}), measured using a Langmuir probe inserted through the plenum view port, with the 1 mm diameter circular disc probe tip biased at −28 V, located on the central axis of the discharge, directly in line with the center of the rf electrode. Using $\frac{n_i}{n_g} = \frac{I_{sat}}{\kappa e v_B A_{LP} n_g}$ where A_{LP} is the area of the Langmuir probe tip and κ is a sheath collection area scaling factor taken as 0.55,[22] the calculated ionization fractions at 1.5 Torr and 10 W were 0.44% for Ar and 0.19% for N_2.

The mean free path (λ) for an ion-neutral charge exchange collision is $\lambda = \frac{1}{n_g \sigma_{CE}}$ where n_g is the neutral gas density and σ_{CE} is the ion-neutral charge exchange collision cross section taken from Phelps[23] as 46 μm in Ar and 40 μm in N_2. This gives the total number of collisions across the discharge diameter as 90 in Ar and 80 in N_2 at 1.5 Torr. However, the cross sections for elastic and ion-neutral charge exchange collisions are approximately equal for both Ar and N_2, meaning half the collisions would be elastic, resulting in 45 and 40 ion-neutral charge exchange collisions across the discharge diameter for Ar and N_2, respectively. Combined with the ionization fraction, an estimated 20% Ar and 8% N_2 neutrals undergo an ion-neutral collision and become hot neutrals in a 1.5 Torr discharge.

For the spatially averaged neutral gas temperature, as measured by the OES method, it is assumed a sufficient number of collisions between hot and cold molecules occur for thermalization of the hot and cold neutral populations. Assuming the majority of neutrals become heated at the location of the rf electrode, there is 10 mm to travel before exiting the discharge volume. Based on the hot neutral temperatures above, the average velocity (v) of hot molecules is $1760\,\mathrm{ms}^{-1}$ and $1533\,\mathrm{ms}^{-1}$ for Ar and N_2, respectively, and $432\,\mathrm{ms}^{-1}$ and $516\,\mathrm{ms}^{-1}$ for cold Ar and N_2, respectively (based on 300 K temperature). Using the average velocity of the hot and cold molecules, to find the time between collisions ($\tau = \frac{1}{n_g \sigma_n v}$ where σ is the neutral-neutral collision cross section) gives approximately 15 thermalizing neutral-neutral collisions at 1.5 Torr for both Ar and N_2 which is sufficient to assume thermalization occurs.

The estimated neutral gas temperatures using this simplified model for Ar and N_2 discharges with pressures from

1 Torr to 4.5 Torr are shown in Figure 3. Measurements of the ion saturation current for pressures less than 1 Torr were not possible in Ar as the discharge could not be maintained at lower pressures with the Langmuir probe in place. For N_2, the discharge could not be maintained for pressures under 2 Torr with the Langmuir probe in place. Instead, the ion saturation currents for 1 and 1.5 Torr in N_2 were estimated using the trend of the remaining results to allow the model to be extended down to 1 Torr for both discharge gases. The model predicts temperatures around 1200 K in Ar and 500 K in N_2 which are slightly higher than but similar to the experimental results, with the Ar temperatures just over 2 times higher than the N_2 temperatures, also in agreement with the experimental results. From the model, the difference between Ar and N_2 temperatures arises from the additional degrees of freedom of N_2 and the ionization fraction of N_2 being just under half the ionization fraction of Ar.

In the Ar model, the predicted temperature drops rapidly from 1200 K at 3 Torr to 780 K at 4.5 Torr. For an Ar discharge with pressures less than 3 Torr, the electron distribution forms a peak on the central axis, but as the pressure increases to over 3 Torr the electron distribution changes to an annular configuration.[6] When measuring the ion saturation current, the Langmuir probe was inserted with the probe tip lying on the central axis. For pressures over 3 Torr, the majority of ions are located in the annular ring with the electrons and not on the central axis, resulting in underestimates of the ion saturation current, hence underestimates of the neutral gas temperature by the model.

To confirm a similar issue is not occurring in the N_2 model, radial intensity profiles across the discharge diameter of the N_2^+ 391nm line were captured using a digital camera in conjunction with a 390 nm filter with 10 nm bandwidth looking through the rear plenum view port, with the results shown in Figure 4 for a 20 W N_2 plasma. Assuming two step ionization, the intensity profile represents n_e^2, where n_e is the electron density. A mode change from a central peak electron density to annular electron density occurs, similar to the Ar discharge, but the mode change occurs at a higher pressure (between 4.8 and 6 Torr), outside the pressures used for the experiment and model, therefore the mode change does not affect the results for the N_2 plasma.

In summary, the neutral gas temperature of an N_2 discharge at 10 W was found to be only slightly higher than the temperature of a cold gas thruster (~300 K) for pressures ranging from 0.5 Torr to 4.5 Torr. However, when using Ar as the discharge gas, with pressures from 0.5 Torr to 4.5 Torr, the neutral gas temperature is between two to three times higher than a cold gas thruster reaching temperatures over 1100 K for 10 W input power. A simplistic model based on collisional and kinetic effects within the discharge was developed, showing the lower temperatures of the N_2 discharges being due to nitrogen gas having a lower ionization fraction compared to argon gas and the additional degrees of freedom in diatomic nitrogen molecules compared to atomic argon molecules. Both the experimental results and the model show that neutral gas heating is occurring within the Pocket Rocket discharge for Ar. Confirmation of neutral gas heating occurring within the discharge for Ar, combined with the low power input, small volume, lack of exposed electrodes and no requirement for an external neutralizer, validates the Pocket Rocket concept as a viable radio-frequency electrothermal plasma micro-thruster.

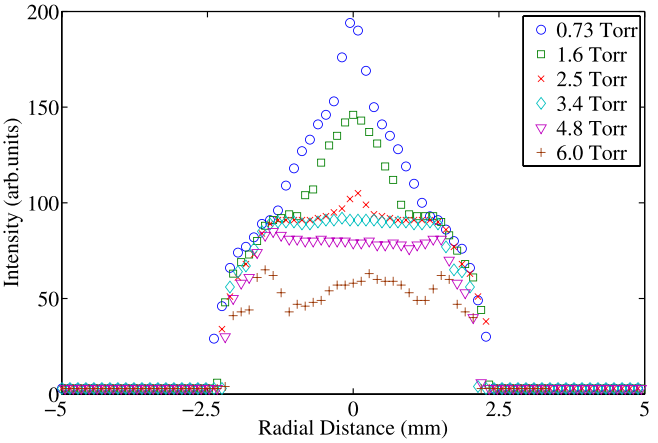

FIG. 4. N_2^+ 391 nm emission line intensity imaged with the digital camera as a function of radial distance (from centerline) of a N_2 plasma for upstream pressures ranging from 0.73 Torr to 6 Torr at 20 W input power.

Aspects of this research made use of software developed by the Inversion Laboratory (ilab). Ilab is part of the Auscope AGOS project—an initiative of the Australian Government funded through the Education Investment Fund.

[1]D. M. Goebel and I. Katz, *Fundamentals of Electric Propulsion: Ion and Hall Thrusters*, edited by J. H. Yuen (John Wiley and Sons, 2008).
[2]C. Charles, J. Phys. D: Appl. Phys. **42**, 163001 (2009).
[3]A. Dunaevsky, Y. Raites, and N. Fisch, Appl. Phys. Lett. **88**, 251502 (2006).
[4]M. Martinez-Sanchez and J. Pollard, J. Propul. Power **14**, 688 (1998).
[5]R. Boswell, C. Charles, P. Alexander, J. Dedrick, and K. Takahashi, IEEE Trans. Plasma Sci. **39**, 2512 (2011).
[6]C. Charles and R. W. Boswell, Plasma Sources Sci. Technol. **21**, 022002 (2012).
[7]C. Charles, R. W. Boswell, and K. Takahashi, Plasma Phys. Controlled Fusion **54**, 124021 (2012).
[8]T. Trottenberg, A. Spethmann, J. Rutscher, and H. Kersten, Plasma Phys. Controlled Fusion **54**, 124005 (2012).
[9]A. Fruchtman, Plasma Sources Sci. Technol. **17**, 024016 (2008).
[10]D. M. Phillips, J. Phys. D: Appl. Phys. **9**, 507 (1976).
[11]M. S. Bak, W. Kim, and M. A. Cappelli, Appl. Phys. Lett. **98**, 011502 (2011).
[12]B. Bai, H. H. Sawin, and B. A. Cruden, J. Appl. Phys. **99**, 013308 (2006).
[13]X.-J. Huang, Y. Xin, L. Yang, Q.-H. Yuan, and Z.-Y. Ning, Phys. Plasmas **15**, 113504 (2008).
[14]H. R. Griem, *Plasma Spectroscopy* (McGraw-Hill Book Company, Inc., 1964).
[15]J. L. Dunham, Phys. Rev. **41**, 721 (1932).
[16]R. Zare, E. Larsson, and R. Berg, J. Mol. Spectrosc. **15**, 117 (1965).
[17]G. Herzberg, *Molecular Spectra and Molecular Structure* (Prentice-Hall, Inc., 1945), Vol. 1.
[18]E. S. Fishburne, J. Chem. Phys. **47**, 58 (1967).
[19]R. Foest, M. Schmidt, and K. Becker. Int. J. Mass Spectrom. **248**, 87 (2006).
[20]N. Masoud, K. Martus, M. Figus, and K. Becker, Contrib. Plasma Phys. **45**, 32 (2005).
[21]A. Meige, O. Sutherland, H. B. Smith, and R. W. Boswell, Phys. Plasmas **14**, 032104 (2007).
[22]T. E. Sheridan, Phys. Plasmas **7**, 3084 (2000).
[23]A. Phelps, J. Phys. Chem. Ref. Data **20**, 557 (1991).